Supporting Information

For

Two Unsupported Terminal Hydroxido Ligands in a μ-Oxo-Bridged Ferric Dimer: Protonation and Kinetic Lability Studies

*Thomas Philipp Zimmermann,[†] Thomas Limpke,[†] Nicole Orth,[§] Alicja Franke,[§] Anja Stammler,[†] Hartmut Bögge,[†] Stephan Walleck,[†] Ivana Ivanovic-Burmazovic,[§] and Thorsten Glaser,[†]**

Fakultät für Chemie, Universität Bielefeld, Universitätsstr. 25, D-33615 Bielefeld, Germany

Department Chemie und Pharmazie, Friedrich-Alexander-Universität Erlangen-Nürnberg, Egerlandstr. 3, D-91058 Erlangen, Germany

thorsten.glaser@uni-bielefeld.de (T. G.)

* To whom correspondence should be addressed.

† *Fakultät für Chemie, Bielefeld*

§ Institut für Anorganische Chemie, Erlangen

Table S1. The values of pK_1 and pK_2 determined at various wavelengths.

Wavelength, nm	**pK_1**	**pK_2**
345	4.91 ± 0.06	6.78 ± 0.09
350	4.98 ± 0.04	6.44 ± 0.17
367	5.2 ± 0.03	7.00 ± 0.25
500	4.69 ± 0.05	6.86 ± 0.06

Figure S1. Thermal ellipsoid plots of the dications a) **$Fe_2(OH)_2^{2+}$** and b) **$Fe_2F_2^{2+}$** in single-crystals of a) [(susan){Fe^{III}(OH)(μ-O)Fe^{III}(OH)}](ClO_4)$_2$ and b) [(susan){Fe^{III}F(μ-O)Fe^{III}F}](ClO_4)$_2$•MeOH, respectively. Hydrogen atoms are omitted for clarity despite the hydrogen atoms of the coordinated OH^- ligands. Thermal ellipsoid are drawn at the 50% probability level.

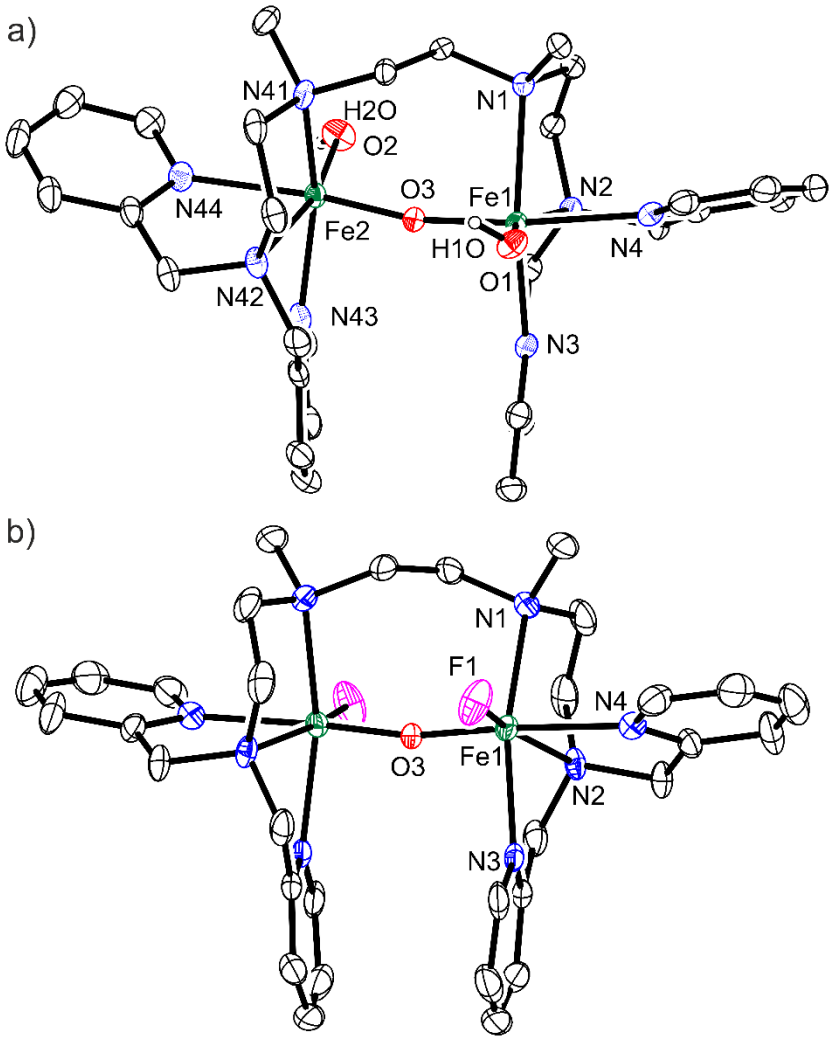

Figure S2. 80 K Mössbauer spectra of a) [(susan){Fe^{III}(OH)(μ-O)Fe^{III}(OH)}]$(ClO_4)_2$ and b) [(susan){Fe^{III}F(μ-O)Fe^{III}F}]$(ClO_4)_2$. Open circles correspond to experimental data and solid lines corresponds to fits using the following parameters: a) blue doublet: δ_1 = 0.45 mm s^{-1}, $|\Delta E_Q|_1$ = 2.00 mm s^{-1}, Γ = 0.28 mm s^{-1}, rel. intensity 49.88 %; red doublet: δ_2 = 0.44 mm s^{-1}, $|\Delta E_Q|_2$ = 1.57 mm s^{-1}, Γ = 0.28 mm s^{-1}, rel. intensity 50.12 %; b) 0.45 mm s^{-1}, $|\Delta E_Q|_1$ = 1.68 mm s^{-1}, Γ = 0.29 mm s^{-1}.

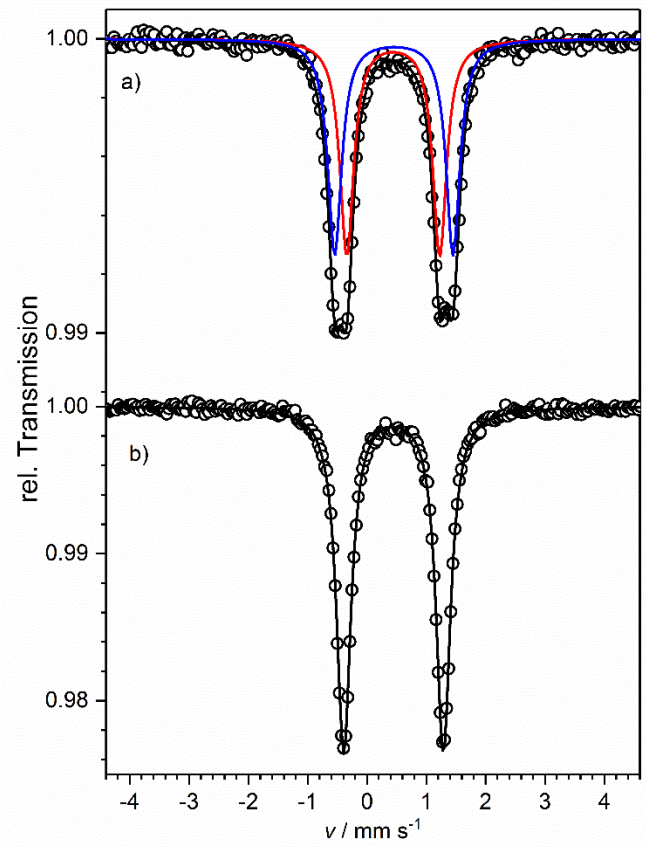

Figure S3. Temperature-dependence of the effective magnetic moment, μ_{eff}, for a) [(susan){Fe^{III}(OH)(μ-O)Fe^{III}(OH)}]$(ClO_4)_2$ and b) [(susan){Fe^{III}F(μ-O)Fe^{III}F}]$(ClO_4)_2$. Open circles correspond to experimental data and solid lines corresponds to simulations using the following spin-Hamiltonian parameters: a) J = - 99.13 cm^{-1}, g = 2.035, p.i.= 0.2% (S = 5/2), Θ_W (p.i.) = - 3.0 K; b) J = - 98.94 cm^{-1}, g = 2.030, χ_{TIP} = 134*10^{-6} cm^{-3} mol^{-1} (subtracted), p.i.= 0.2% (S = 5/2), Θ_W (p.i.) = - 7.0 K.

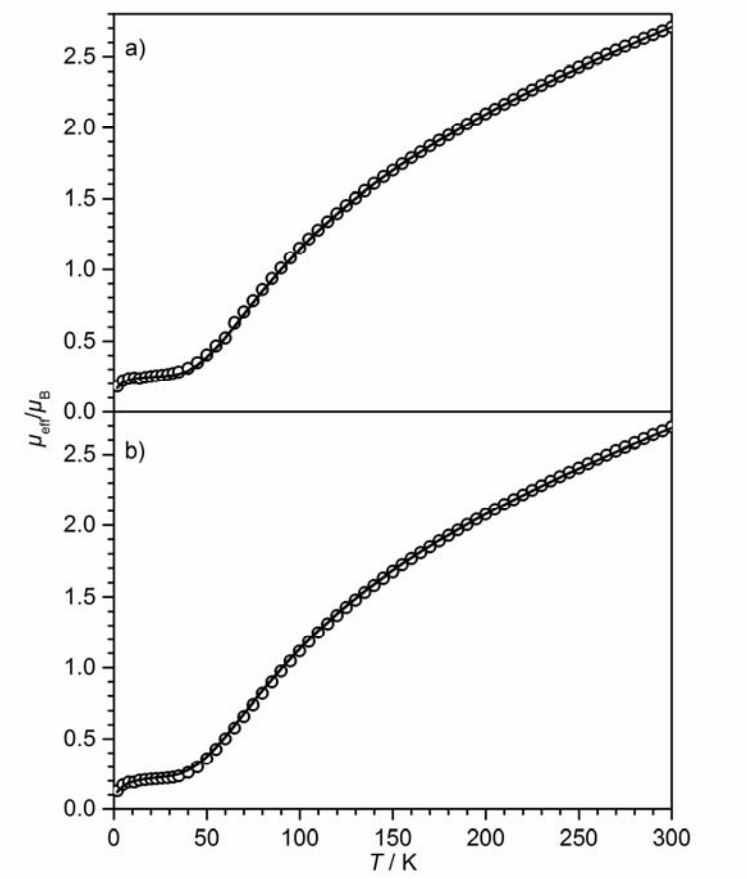

Figure S4. 80 K Mössbauer spectra of CH_3CN solution of a) [(susan){Fe^{III}(OH)(μ-O)Fe^{III}(OH)}]$(ClO_4)_2$, b) after addition of 1 equivalent of $HClO_4$ at -40°C, and c) after addition of 2 equivalents of $HClO_4$ at -40°C. Open circles correspond to experimental data and solid lines corresponds to fits using the parameters provided in the figure.

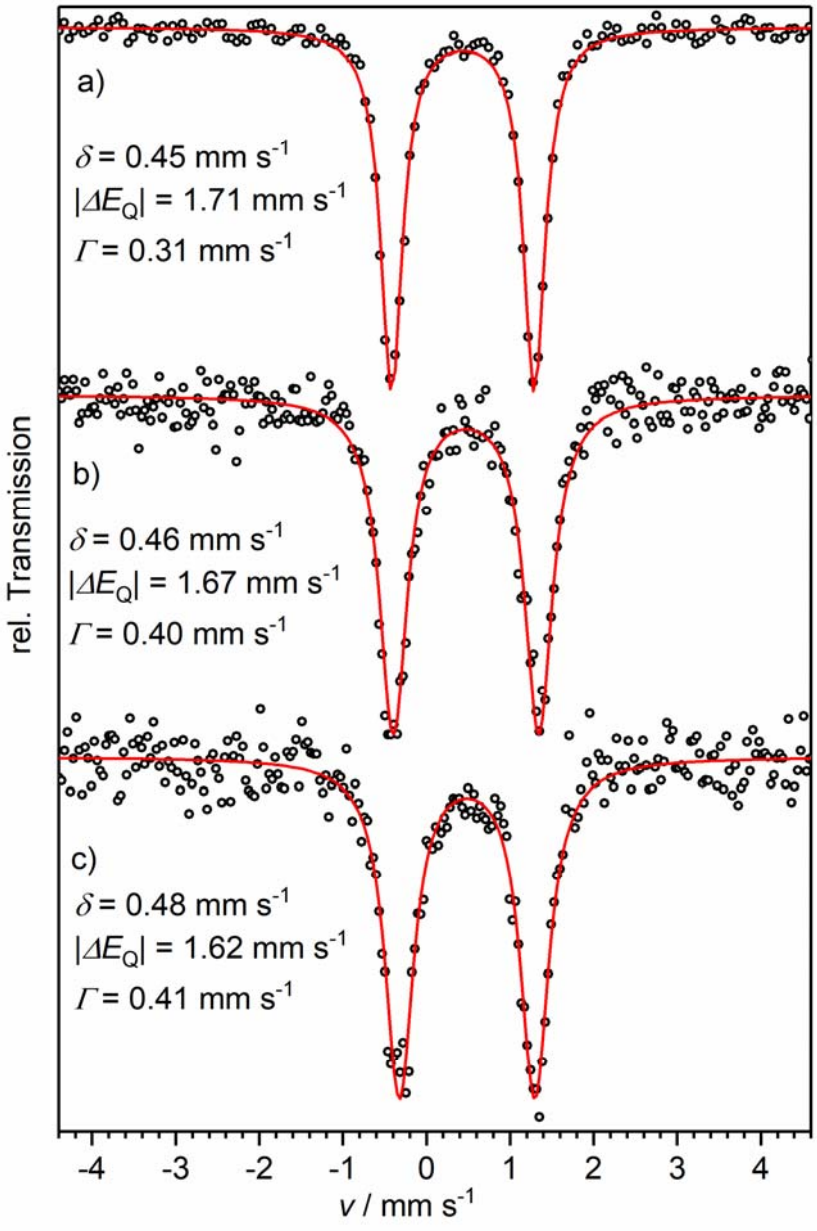

Figure S5. UV-vis spectral changes observed for aqueous solutions of $\mathbf{Fe_2(OH)_2^{2+}}$ in the range of pH 3.8-9.9. Inset: Spectral changes from 27000 to 30000 cm^{-1} showing two sets of isosbestic points. Experimental conditions: $c(\mathbf{Fe_2(OH)_2^{2+}})$ = 4 × 10^{-5} M, 25 °C, I = 0.1 M (adjusted with $NaClO_4$).

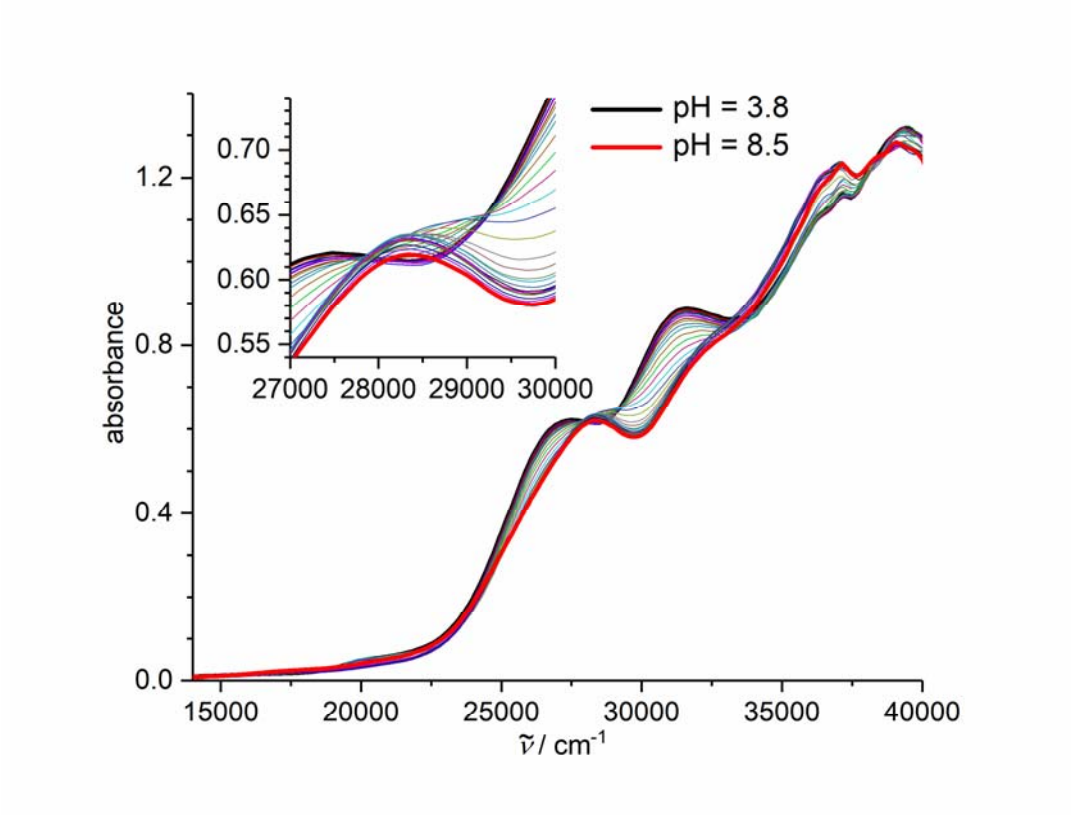

Figure S6. pH-Dependence of the absorbance at 29000 (a), 28570 (b), 27250 (c) and 20000 (d) cm^{-1}. Solid lines are simulations to the equation for two protonation steps with Δ pH ≤ 3. Experimental conditions: see Figure S5.

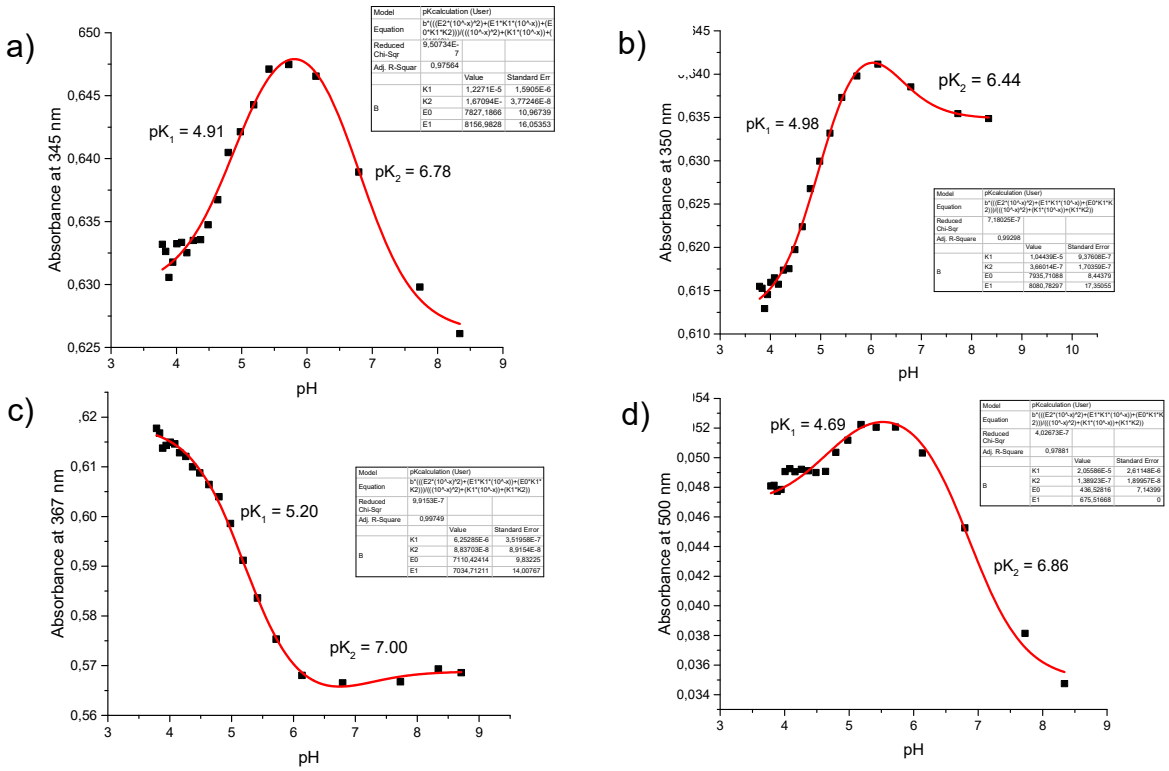

Fig. S7. UHR-ESI-MS spectra and their simulations (below) recorded for $\mathbf{Fe_2(OH)_2^{2+}}$ (5×10^{-4} M) in water at pH = 2.5 at positive mode at 5 °C.

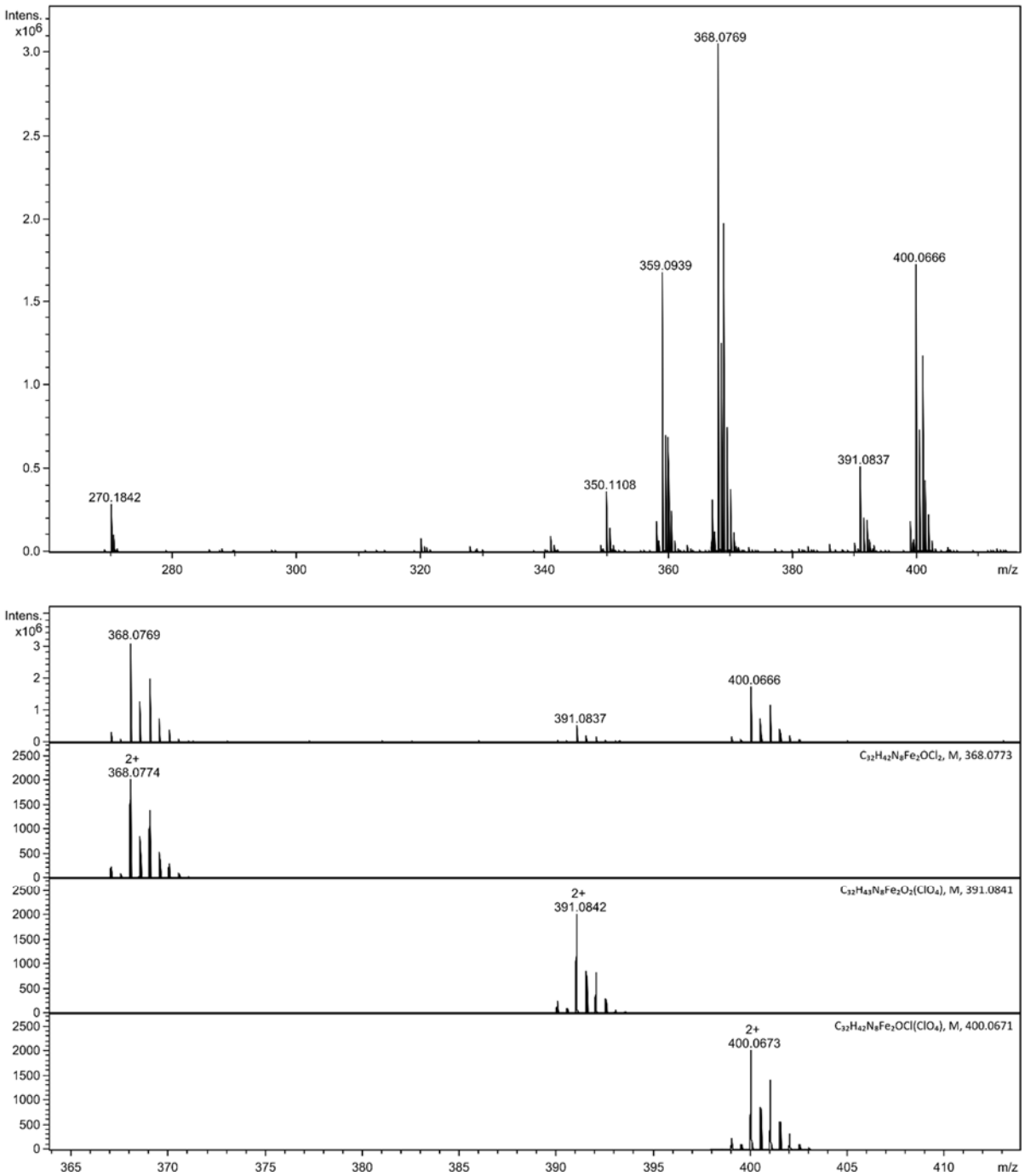

Fig. S8. UHR-ESI-MS spectra and their simulations (below) recorded for **$Fe_2(OH)_2^{2+}$** (5×10^{-4} M) in water at pH = 3.3 at positive mode at 5 °C.

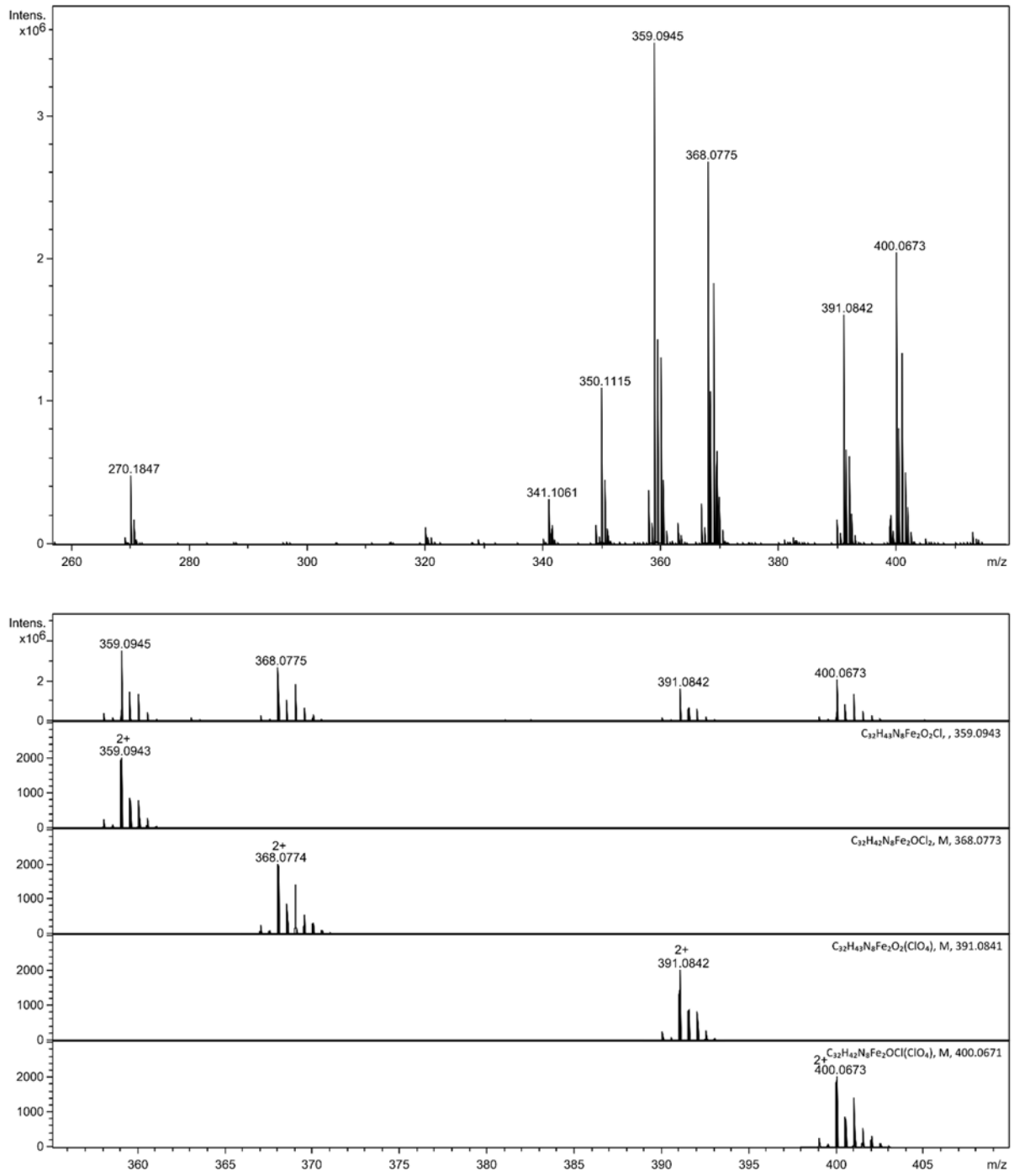

Fig. S9. UHR-ESI-MS spectra and their simulations (below) recorded for $\mathbf{Fe_2(OH)_2^{2+}}$ (5×10^{-4} M) in water at pH = 6.0 at positive mode at 5 °C.